

# On the Existence of Electronic States Confined by Charged Groups in Proteins

Felipe Aparicio,<sup>†</sup> Joel Ireta,<sup>†,‡</sup> Arturo Rojo,<sup>†</sup> Laura Escobar,<sup>§</sup> Andrés Cedillo,<sup>†</sup> and Marcelo Galván<sup>\*,†</sup>

Departamento de Química, Universidad Autónoma Metropolitana-Iztapalapa, A.P. 55-534, México, D.F. 09340, México, and Departamento de Fisiología, Facultad de Medicina, Universidad Nacional Autónoma de México, México D.F., México

Received: July 9, 2002; In Final Form: October 18, 2002

The electronic structure of the peptidic BgK toxin is obtained at an ab initio level with the total energy pseudopotential method using a plane wave basis expansion. A detailed analysis of the electronic structure reveals the existence of electronic unoccupied states in structural cavities generated by the particular folding of the polypeptide. The existence of such kind of electronic states is verified using different structural models of the system and employing different levels of theory. Finally, the stability upon occupation of this kind of states is determined as well as the influence of polar solvents.

## Introduction

The great complexity of polypeptide chains includes the existence of regular secondary structure, such as alpha helix and beta sheet, as well as the association of subunits and the possibility of covalent cross-linking bonds, namely, disulfide bridges.<sup>1</sup> Also, these complex systems have interstitial regions which are atom-less zones surrounded by specific functional groups. These interstitial regions can be found as internal cavities or surface invaginations and may play interesting roles from the electronic structure point of view. In addition, the presence of charged groups gives rise to different possible situations: interstitial regions surrounded by positive, negative, or a mixture of positive and negative functional groups.<sup>2</sup> It is generally considered that electrostatic interactions between charged groups play an important role in determining the structure and functions of proteins in a wide variety of cellular and biochemical processes.<sup>3</sup> There are several proteins where charged group pairs are located in close contact, and the stability of these systems has been studied.<sup>4</sup> The present work focuses on the description of the electronic-structure characteristics of an interstitial region surrounded by positively charged groups.

Because this study requires the evaluation of the electronic structure of such a region in a polypeptide, several restrictions must be considered: the polypeptide has to be small enough so that the estimation of the electronic structure as a whole is feasible; the experimental atomic geometry has to be known to avoid the search for the equilibrium conformation of the macromolecule and focus on the electronic structure; and the polypeptide should have charged groups in appropriate conformation.

There is a family of polypeptides that satisfy the above criteria: the toxins that have a high affinity for potassium channels.<sup>5</sup> These toxins have been isolated from snakes, scorpions, cone snails, and sea anemones for structure–function

studies on voltage-gated potassium channels (Kv), in particular the Kv1 subfamily.<sup>6,7</sup> The Kv channels regulate cellular processes by controlling membrane potential and electrical excitability.<sup>8</sup> Despite their limited selectivity for a given Kv1 subtype, these blockers exert their function by binding in one-to-one stoichiometry to the same P region of the channels.<sup>5</sup> The binding sites of all of these toxins contain a conserved pair of functional residues, lysine and an aromatic amino acid, separated by 6.6 Å.<sup>9</sup>

Potent blockers endowed with high selectivity toward these channels would be of great interest. For example, homomeric Kv1.3 channels in T-lymphocytes are being considered as a therapeutic target for immunosuppression.<sup>10</sup>

For the present study, the BgK toxin from *Bundosoma granulifera* was selected.<sup>11</sup> This toxin allowed us to show the existence of electronic states localized in an interstitial region. Because these states are among the lower unoccupied ones, their possible role in the chemical reactivity of the macromolecule is analyzed.

## The BgK Toxin

BgK belongs to a class of toxins that binds to dendrotoxin-sensitive K<sup>+</sup> channels.<sup>5</sup> This 37 amino acid polypeptide has a basic isoelectric point and a net charge of +5 because of the existence of three negatively and eight positively charged side chains in addition to the amino (positive) and carboxylic (negative) endings. Its backbone structure contains two helices running from residues 9–16 and 24–31, and three disulfide bridges between residues 20–34, 11–30, and 2–37.<sup>9</sup> These structural features of BgK produce a rigid and closely packed globular shape. The rigid architecture of the toxin is mainly due to the disulfide bridges, one of them linking the two helices. A general view of the molecule is presented in Figure 1. Six out of the fifteen NMR structures reported in ref 9 maintain two amino acids, Arg21 and Arg27, close enough that some of the hydrogen atoms attached to the corresponding guanidinium groups are around 3 Å far from each other, as it is shown in the Figure 2. We selected one of those structures to perform our study.<sup>12</sup>

\* To whom correspondence should be addressed. Phone: (525)-804-6413. Fax: (525)-804-4666. E-mail: mgalvan@xanum.uam.mx.

<sup>†</sup> Universidad Autónoma Metropolitana-Iztapalapa.

<sup>‡</sup> Present address: Fritz-Haber-Institut der Max-Planck-Gesellschaft, Faradayweg 4–6, D-14195 Berlin-Dahlem, Germany.

<sup>§</sup> Universidad Nacional Autónoma de México.

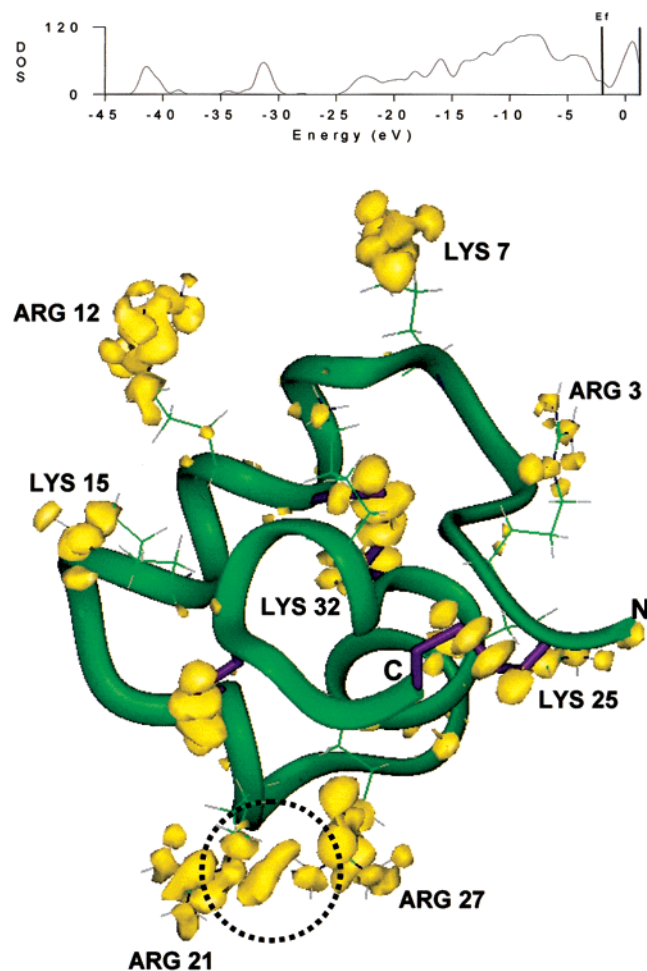


**Figure 1.** Density of states (DOS), structure, and LUMO band of the BgK toxin. The DOS is displayed in the top panel. Ef indicates the Fermi level and the LUMO band is the peak at the right. In the lower panel, the structure of the toxin is presented; it was obtained from the Protein Data Bank.<sup>12</sup> The amino acid sequence is VCRDWFKET-ACRHA KSLGNCRTSQKYRANCAKTCEL C. To have several points of reference in the structure, the positively charged amino acids are labeled and their lateral chains are rendered with sticks; also, the amino and carboxylic endings are marked by N and C letters, respectively; the disulfide bridges are rendered with purple sticks. The region marked by a dashed circle is the one this work focuses on, and it contains the interstitial state. An isosurface of the accumulated orbital density for the LUMO band containing 30 states, as calculated with a plane wave expansion using a 6 Ry cutoff, is displayed in yellow; this isosurface was created using a value, in atomic units, of 0.1.

### Methodology

To have a qualitative description of the electronic structure of the toxin as a whole, density functional theory (DFT) single-point calculations were performed. The program used was a Silicon Graphics implementation of the code developed by Joannopoulos et al.<sup>13</sup> The plane wave expansion was set using an energy cutoff of 6 Ry,<sup>14</sup> and the local density approximation (LDA) was used.<sup>15</sup> The Kohn–Sham equations were solved with the method developed by Arias et al.<sup>16</sup> For the present case, a  $26.6 \times 23.3 \times 27.0$  Å supercell was used to fulfill the condition that the minimum distance between molecules in neighbor cells is of 5 Å.<sup>17</sup> The last condition was satisfied by all of the supercells used in this work. This approach only considers the valence electrons; accordingly, the pseudopotentials were produced following the prescription developed by Rappe et al using a 40 Ry cutoff.<sup>18</sup> The details of the performance of the 6 Ry cutoff plane wave expansion to describe the outer parts of the density can be found in refs 19 and 20.

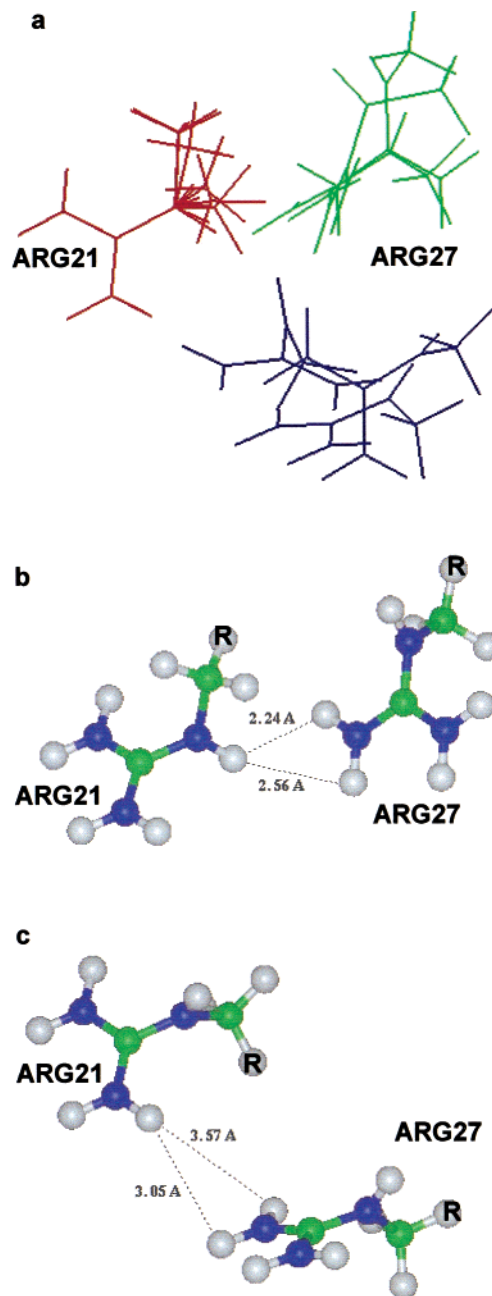


**Figure 2.** Conformation of Arg21 and Arg27 in the six NMR structures of BgK, in which the interstitial state is present. (a) Superposition of the six structures, taking the guanidinium group of Arg21 as a point of reference. Among them, there are two structural regimes exemplified by panels b and c. The panel b shows the structure 1 of the NMR set, which is an example of the structures shown in panel a where Arg27 is presented in green. The panel c shows an example of the structures represented in blue, and it corresponds to the structure 6 of the NMR set. The BgK structures were simplified by removing all of the atoms beyond the site marked with letter R. The corresponding bond was saturated with a hydrogen atom.

We now focus on the analysis of a region, influenced by two arginine residues, that is not a bonding nor an atomic zone. This part of the macromolecule is circled in Figure 1. For such a region, one can expect that plane waves, as a naturally delocalized basis set, give a suitable description. However, when the plane wave expansion is truncated, one should expect a poor description of the regions close to the nuclei because in these regions density increases rapidly. To verify that the 6 Ry plane wave truncation is not producing spurious results in the present case, several tests were performed. A calculation was done for

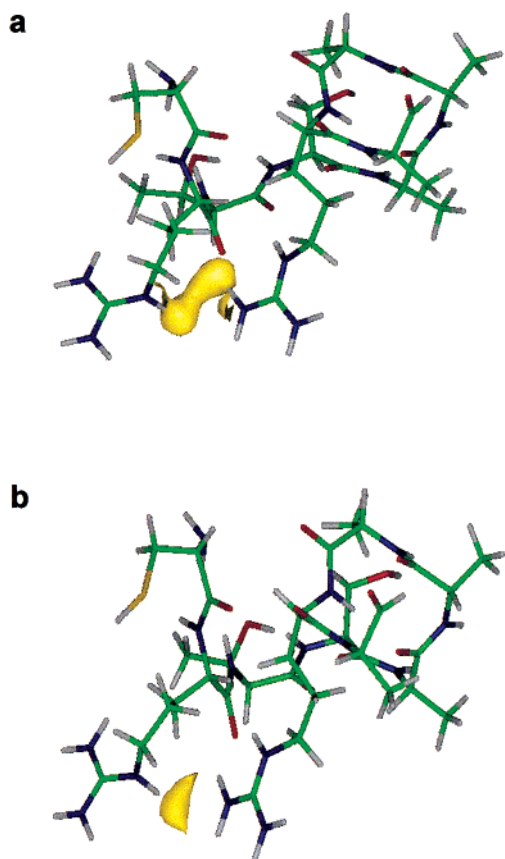


**Figure 3.** Isosurfaces of the LUMO band for the seven residues fragment, Arg21 to Arg27, of BgK. The values of the isosurfaces, in atomic units, are 0.15 for both cases. The calculations were done with (a) the total energy pseudopotential method with a plane wave expansion truncated by an energy cutoff of 20 Ry; and (b) with the B3LYP/6-31G\*\* method. The fragment sequence was simplified from RTSQKYR to RAAAAAR without relaxing the backbone geometry. The condensed formula and charge are, respectively,  $C_{27}H_{53}O_8N_{13}$  and +2.

a fragment of seven amino acids; in this calculation, frozen coordinates were used, and the corresponding dangling bonds were passivated to simulate complete amino acids (see Figure 3). This calculation used a plane wave expansion, truncated up to a 20 Ry cutoff, which is good enough to produce a reliable description of the inner and outer parts of the valence charge density;<sup>19,20</sup> for this fragment, a supercell of  $15.9 \times 12.4 \times 16.7$  Å was used. On the other hand, a different test was done using a localized basis set at the B3LYP/6-31G\*\*<sup>21,22</sup> level of theory within the Gaussian 98 program.<sup>23</sup> The rationale of this calculation was to use a well tested exchange and correlation functional beyond the LDA approximation and a standard localized basis set without diffuse functions. If one has a similar qualitative description of the region of interest with both, the fully diffuse basis set and the reliable localized basis set, then one can be more confident with the results obtained with the plane wave calculation.

## Results

**Interstitial Empty States.** The analysis of the density of states (DOS) of BgK toxin (top panel in Figure 1) reveals a similar pattern as the previously obtained for a scorpion toxin<sup>19</sup> and for nanotubes built from amino acids.<sup>24</sup> In systems such as solids, polymers, and surfaces, the frontier orbital concept, which is useful in a chemical reactivity analysis, is extended to that of the frontier bands;<sup>25</sup> this extension has shown to be useful in the analysis of the electronic structure of proteins.<sup>26</sup> In the BgK

toxin case, the first band of unoccupied states (the LUMO band) has a bandwidth of 3.1 eV, and its integration gives a total of 30 states. Many of them are localized around the positive amino acids; also, some states are localized in the disulfide bond regions (Figure 1). The yellow surface in Figure 1 surrounds regions where the orbital density is larger than 0.1 au. This value is good enough to describe the regions where the orbital density is mainly localized.

The striking feature of the local behavior of the LUMO band is that there is an accumulation of orbital density between two positively charged residues indicated by a dashed circle in Figure 1. These charged amino acids are kept close to each other (the closest atoms are about 2.2 Å apart) by the particular folding of the toxin, forming a small interstitial site among them. The isosurface plot of the LUMO band shows that the orbital density is located in an atom-less zone within such interstitial site, which does not correspond to a bonding region. As one can see in Figure 2, it is important to notice that in this site no hydrogen bonds are found, according to the standard criteria.<sup>27</sup>

The behavior of the interstitial LUMO orbital density for a fragment containing seven amino acids, starting in Arg21 and finishing in Arg27 of the sequence, is shown in Figure 3 and one can see that the interstitial state appears in both types of calculations. Thus, the existence of such a state is not an artifact of the plane wave expansion because it is also predicted by a localized basis set. It is important to mention that the interstitial state is also present when the calculation is done at the HF/6-31G\*\* level of theory.

**Influence of Occupation on the Interstitial State.** The behavior of unoccupied states is the result of the self-consistent-field of an effective Kohn–Sham potential generated by the occupied states. Consequently, in contrast to an occupied state, they are not under the influence of the Coulombic repulsions nor of the exchange and correlation interactions. These effects could change the local behavior of the state, particularly, if it is localized far from the influence of the nuclei. One way of addressing this situation consists of occupying the state and to analyze the changes induced when the interactions are turned on. For this analysis, a calculation of a model containing only the two charged residues that are related to the formation of the interstitial state, Arg21 and Arg27, was performed. The study was done at two levels of theory: B3LYP/6-31G\*\* and LDA/pseudopotentials/plane waves at 20 Ry cutoff/supercell of  $10.3 \times 12.6 \times 13.1$  Å. To be consistent with a reactivity study based on bands rather than in single states, the analysis of the unoccupied orbitals includes those with eigenvalues in the range of 2 eV above the LUMO. For both cases, the first and second unoccupied Kohn–Sham orbitals are degenerated, and an isosurface orbital density map shows that they are localized in the guanidinium groups of arginine residues; in addition, the interstitial state corresponds to the third unoccupied Kohn–Sham orbital. It is important to mention that this state has a similar local behavior as the corresponding from the seven amino acids model. To occupy this state, a calculation for the two amino acids model was set up: the plane wave expansion was truncated by a 20 Ry cutoff and six extra electrons were included to ensure the occupation of the interstitial state. The new system has a total charge of −4, and for this anionic system, the HOMO corresponds to the interstitial state. A contour plot of the orbital density of the HOMO state for the anionic system is presented in Figure 4. The plane of the plot contains the three hydrogen atoms located in the region of interest. In the figure, it is clear that the orbital is mainly localized in the interstitial



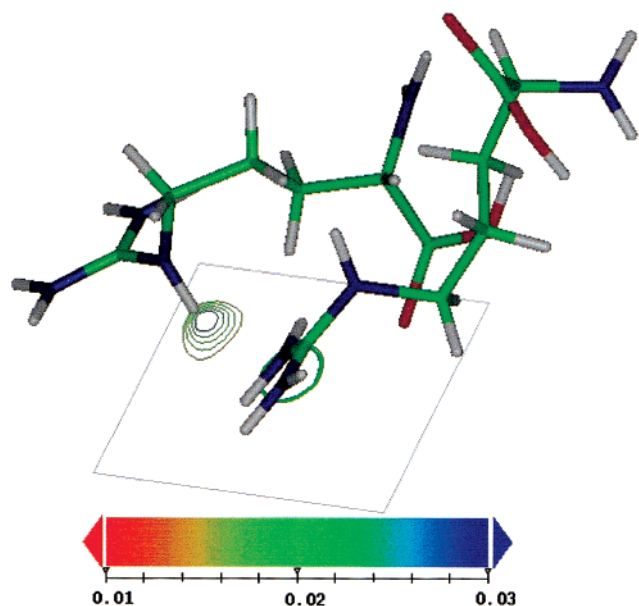


**Figure 4.** Contour plot of the orbital density of the HOMO for a two amino acids model, Arg21 and Arg27, calculated with six additional electrons. The geometry was fixed in the original position in the complete toxin. The condensed formula and charge are, respectively,  $C_{12}H_{30}O_4N_8$  and  $-4$ . The calculation was done with total energy pseudopotential method using a 20 Ry energy cutoff. The plane for the contour plot is defined by the three hydrogen atoms close to the interstitial region. The values of the contours, in atomic units, are 0.015, 0.017, 0.019, 0.021, and 0.023.

region indicating that electron–electron interactions involving this state will not change significantly its local behavior.

**Solvent Effects.** The experimental geometry used in the present study corresponds to a solvated species because it comes from NMR experiments. Therefore, it is important to simulate the effects on the electronic structure from the presence of the solvent. For this goal, a reaction field calculation using the polarized continuum model (PCM)<sup>28</sup> was performed for the structure of Figure 4, with  $+2$  charge at the B3LYP/6-31G\*\* level of theory, using the dielectric constant of water within the Gaussian 98 program. In Figure 5, the local behavior of the interstitial empty state obtained within the reaction field is compared with the one calculated in the vacuum; once again, it is located in the same region showing only some quantitative differences. In addition, the eigenvalue of this state is shifted toward lower values by 0.6 eV. This additional stabilization comes from the presence of a polar solvent, and it affects all of the states in a different amount.

## Discussion

The electronic-structure calculation of the BgK toxin shows that the LUMO band is mainly localized around positive charged groups. The point to stress about LUMO band is the presence of states, close to the Fermi level of the peptide, that exhibit localization around an interstitial region. This region is surrounded by positive charges, and we found that the charges induce a stabilization of the unoccupied states close to them, independently on the level of theory that is used. It seems that the delocalization of the positive charge in the side chains of Arg21 and Arg27 generates a potential that stabilizes empty states inside this region. As it was pointed out in the Introduction, the BgK toxin binds to the external mouth of the potassium channel, which contains several negatively charged groups.<sup>29</sup> Thus, in the interaction between the channel and the toxin, the charge transfer process could involve negatively charged species

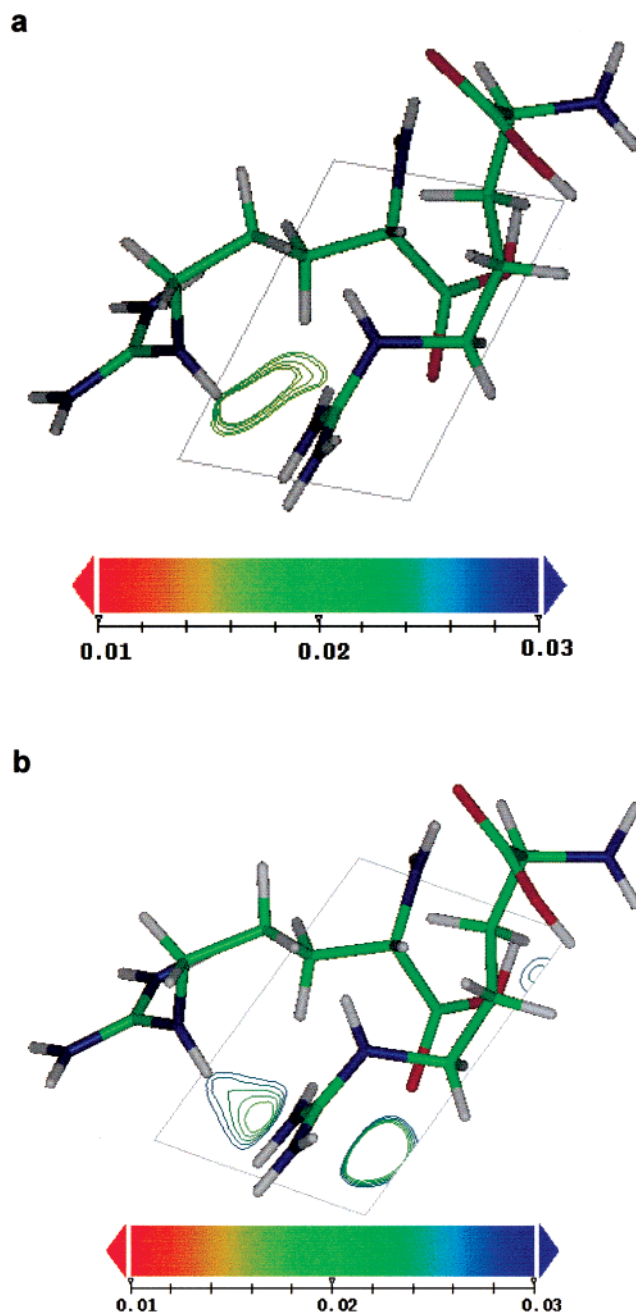


**Figure 5.** Comparison of the local behavior of the interstitial state in the vacuum and in the presence of a polar solvent. The contour plots are on a plane similar to that of Figure 4. The top panel corresponds to the calculation in the vacuum. In the lower panel, the water medium was simulated by a reaction field.<sup>28</sup> The contour values for both panels in atomic units are 0.020, 0.022, 0.024, 0.026, and 0.028.

and empty states. Because the interstitial state is among the first Kohn–Sham orbitals above the Fermi level of the toxin, and it is accessible because it is located in the external part of the toxin, it can be implicated in an interaction with several contact sites. In this context, it is important to notice in Figure 4 that the interstitial nature of the state is not triggered by the possibility of occupation. Even though it has not been experimentally demonstrated yet, charge transfer may exist during the toxin–channel interaction; if so, the interstitial site could be involved in this process. In this sense, the preservation of the interstitial state would be relevant.

The shifting effect of polar solvents on the orbital energies of proteins has been recently documented.<sup>26</sup> In the present work, a similar shifting was observed; however, as it is seen in Figure

5, the local behavior of the interstitial state remains qualitatively unchanged in the presence of a polar solvent.

The description of the interstitial empty state could be endangered by the incorrect asymptotic behavior of the LDA Kohn–Sham potential. However, we corroborate that the qualitative behavior is preserved when the Hartree–Fock method, which has the appropriate asymptotic comportment, is used.

A direct chemical implication of the presence of the unoccupied states described above is the enhancement of the electrophilic character of a region such as the one marked by the circle in Figure 1. This is due to the fact that, in addition to the unoccupied states localized in atomic sites, there is another state, an interstitial one, available for charge-transfer processes, generated by the cumulative effect of several positive charges in the same region.

The results presented in this work suggest the importance to analyze regions of the size of amino acids and to look for schemes in which one could include interstitial regions. To clarify this issue, one may think in a standard population analysis to assign reactivity behavior. It is evident that, without locating floating orbitals in the appropriate positions, one may lose the contribution of states localized in cavities such as the one described in this work. In general, a plane wave basis set or a localized one with floating orbitals are recommended to achieve an appropriate description of interstitial states.

The analysis of dynamical aspects on the interstitial states is beyond the scope of the present work. To begin exploring along this direction, the LUMO orbital densities of the six structures presented in Figure 2 were calculated at the B3LYP/6-31G\*\* level of theory, showing the existence of an interstitial state in all of them. The fact that some of the BgK experimental structures can develop interstitial states indicates that thermal fluctuations could allow their formation. Whether the existence of the interstitial state in BgK is just a single case feature or a characteristic of closely packed globular proteins with several positive charges is a question whose solution requires future work. Up to now, we have identified this feature, in addition to BgK, in charybdotoxin another toxin but isolated from scorpion venom.<sup>30</sup> For charybdotoxin, the interstitial state is located in an internal region close to Lys27 and Arg34. These two molecules belong to a family of toxins consisting of small and compact polypeptides containing charged groups and several disulfide bridges, having many structural restrictions. This would be a kind of system where it is expected to find interstitial regions such as the one studied in this work. To define the minimum conditions required to develop interstitial states is not feasible from the findings of the present work; however, our group is working along this line with simpler structural models.

To this point, it is important to mention that electrostatic interactions play a central role in the determination of protein structure and function.<sup>3</sup> The investigations on electrostatic interactions in proteins are mainly based on classical electrostatic formalism.<sup>31</sup> This classical treatment has reached a good level of confidence.<sup>32–35</sup> For example, the electrostatic interactions of a pair of positively charged arginine side chains have been studied.<sup>2,4,36–39</sup> Such pairs can be observed in many proteins, in particular in their solvent accessible regions, and they have proven to play a significant role in the structure and stability of proteins.<sup>40</sup> Nevertheless, some phenomena like the interstitial states cannot be described by a classical approach, because it comes from the electronic distribution of the molecule. This information can only be obtained from a quantum mechanical

treatment because it includes the electrostatic effects, among all of the other interactions.

It was pointed out, that the biological activity of this family of toxins is related to the electrophilic nature of the macromolecule because it interacts with a system rich in electrons: the external mouth of a K<sup>+</sup> channel.<sup>19</sup> Whether the existence of this extra electrophilic character of the toxin is relevant to the biological activity or not is an open question that our group is currently addressing by studying several mutant toxins. Besides, the existence of interstitial states could be of impact in other properties of proteins such as fotoconductivity and electron transport.

Finally, the analysis of the LUMO band, as it is displayed in Figure 1, reveals an interesting point related to the chemical reactivity of proteins: the strong electrophilic character of disulfide bridges. This explains the strong lability of disulfide bridges to reduction processes.<sup>41</sup>

### Concluding Remarks

The existence of interstitial states in proteins is established for the case of positively charged regions in compact structures. These states will influence the electrophilicity of the corresponding proteins. This situation suggests that, in order to get a complete picture of the chemical reactivity of polypeptides, it is worth analyzing the interstitial regions. Furthermore, it is stressed the necessity of performing the analysis in a size scale which does not necessarily match the scale of organic functional groups.

To study the electronic structure of proteins in the search for interstitial states, the use of plane wave basis sets or the addition of floating orbitals to standard localized basis sets is recommended. It is important to notice that plane wave basis sets, at low cutoff energies, qualitatively describe the electronic structure of interstitial regions in proteins; a fact that significantly reduces the computer effort required to search for these features in such complex systems.

**Acknowledgment.** This work received financial support from CONACYT (México) through Contracts 36482-E, 30570-M, and 29124-E. We thank DGSCA at UNAM and Laboratorio de Visualización y Cómputo Paralelo at UAM-Iztapalapa for giving us access to their computer facilities. F.A. and J.I. thank CONACYT for PhD scholarships. A.R. thanks the Third World Academy of Sciences for support through project 98-252RG/CHE/LA.

### References and Notes

- (1) Branden, C.; Tooze, J. *Introduction to Protein Structure*, 2nd ed.; Garland Publishing Inc.: New York, 1999.
- (2) No, K. T.; Nam, K.-Y.; Scheraga, H. A. *J. Am. Chem. Soc.* **1997**, *119*, 12917.
- (3) Perutz, M. F. *Science* **1978**, *201*, 1187.
- (4) Magalhaes, A.; Maigret, B.; Hoflack, J.; Gomes, J. N.; Scheraga, H. A. *J. Protein Chem.* **1994**, *13*, 195.
- (5) Miller, C. *Neuron* **1995**, *15*, 5.
- (6) Chandy, K. G.; Gutman, G. A. *Handbook of Receptors and Channels*; CRC Press: Boca Raton, FL, 1995; pp 1–71.
- (7) Jan, L. Y.; Jan, Y. N. *Annu. Rev. Neurosci.* **1997**, *20*, 91.
- (8) Hille, B. *Ionic Channels of Excitable Membranes*; Sinauer Associates Inc.: Sunderland, MA, 1992; pp 115–127.
- (9) Dauplais, M.; Lecoq, A.; Song, J.; Cotton, J.; Jamin, N.; Gilquin, B.; Roumestand, C.; Vita, C.; de Medeiros, C. L.; Rowan, E. G.; Harvey, A. L.; Ménez, A. *J. Biol. Chem.* **1997**, *272*, 4302.
- (10) Chandy, G. K.; Cahalan, M.; Pennington, M.; Norton, R. S.; Wulff, H.; Gutman, G. A. *Toxicon* **2001**, *39*, 1269.
- (11) Aneiros, A.; García, I.; Martínez, J. R.; Harvey, A. L.; Anderson, A. J.; Marshall, D. L.; Engstrom, A.; Hellman, U.; Karlsson, E. *Biochim. Biophys. Acta* **1993**, *1157*, 86.

- (12) The structure corresponds to the first of the 15 deposited structures in the Protein Data Bank (<http://www.pdb.org>) for BgK toxin with code 1BGK.
- (13) Payne, M. C.; Teter, M. P.; Allan, D. C.; Arias, T. A.; Joannopoulos, J. D. *Rev. Mod. Phys.* **1992**, *64*, 1045.
- (14) Within the methodology reported in ref 13, commonly the unit Rydberg (Ry) is used to express the energy-cutoff parameter. 1 Ry = 0.5 Hartree.
- (15) Parr, R. G.; Yang, W. *Density Functional Theory of Atoms and Molecules*; Oxford University Press: New York, 1989; pp 142–168.
- (16) Arias, T. A.; Payne, M. C.; Joannopoulos, J. D. *Phys. Rev.* **1992**, *B45*, 1538.
- (17) Rappe, A.; Joannopoulos, J. D.; Bash, P. A. *J. Am. Chem. Soc.* **1992**, *114*, 6466.
- (18) Rappe, A.; Rabe, K.; Kaxiras, E.; Joannopoulos, J. D. *Phys. Rev.* **1990**, *B41*, 1227.
- (19) Ireta, J.; Galván, M.; Cho, K.; Joannopoulos, J. D. *J. Am. Chem. Soc.* **1998**, *120*, 9771.
- (20) Ireta, J.; Galván, M. *J. Chem. Phys.* **1996**, *105*, 8231.
- (21) Becke, A. D. *J. Chem. Phys.* **1993**, *98*, 1372.
- (22) Becke, A. D. *J. Chem. Phys.* **1993**, *98*, 5648.
- (23) Frisch, M. J.; Trucks, G. W.; Schlegel, H. B.; Scuseria, G. E.; Robb, M. A.; Cheeseman, J. R.; Zakrzewski, V. G.; Montgomery, J. A., Jr.; Stratmann, R. E.; Burant, J. C.; Dapprich, S.; Millam, J. M.; Daniels, A. D.; Kudin, K. N.; Strain, M. C.; Farkas, O.; Tomasi, J.; Barone, V.; Cossi, M.; Cammi, R.; Mennucci, B.; Pomelli, C.; Adamo, C.; Clifford, S.; Ochterski, J.; Petersson, G. A.; Ayala, P. Y.; Cui, Q.; Morokuma, K.; Malick, D. K.; Rabuck, A. D.; Raghavachari, K.; Foresman, J. B.; Cioslowski, J.; Ortiz, J. V.; Stefanov, B. B.; Liu, G.; Liashenko, A.; Piskorz, P.; Komaromi, I.; Gomperts, R.; Martin, R. L.; Fox, D. J.; Keith, T.; Al-Laham, M. A.; Peng, C. Y.; Nanayakkara, A.; Gonzalez, C.; Challacombe, M.; Gill, P. M. W.; Johnson, B. G.; Chen, W.; Wong, M. W.; Andres, J. L.; Head-Gordon, M.; Replogle, E. S.; Pople, J. A. *Gaussian 98*, revision A.7; Gaussian, Inc.: Pittsburgh, PA, 1998.
- (24) Carloni, P.; Andreoni, W.; Parrinello, M. *Phys. Rev. Lett.* **1997**, *79*, 761.
- (25) Hoffmann, R. *Solids and Surfaces, A Chemist's View of Bonding in Extended Structures*; VCH Publishers: New York, 1988; pp 5–55.
- (26) Ohno, K.; Kamiya, N.; Asakawa, N.; Inoue, Y.; Sakurai, M. *J. Am. Chem. Soc.* **2001**, *123*, 8161.
- (27) Jeffrey, G. A. *An Introduction to Hydrogen Bonding*; Oxford University Press: New York, 1997; pp 11–32.
- (28) Miertus, S.; Scrocco, E.; Tomassi, J. *Chem. Phys.* **1981**, *55*, 117.
- (29) Anderson, C.; MacKinnon, R.; Smith, C.; Miller, C. *J. Gen. Physiol.* **1988**, *91*, 317.
- (30) Miller, C.; Moczydlowski, E.; Latorre, R.; Phillips, M. *Nature* **1985**, *313*, 316.
- (31) Honig, B.; Nicholls, A. *Science* **1995**, *268*, 1144.
- (32) Lee, L. P.; Tidor, B. *J. Chem. Phys.* **1997**, *106*, 8681.
- (33) Wang, J.; Cieplak, P.; Kollman, P. A. *J. Comput. Chem.* **2000**, *21*, 1049.
- (34) Wang, W.; Donini, O.; Reyes, C. M.; Kollman, P. A. *Annu. Rev. Biophys. Biomol. Struct.* **2001**, *30*, 211.
- (35) Kumar, S.; Nussinov, R. *Chembiochem* **2002**, *3*, 604.
- (36) Boudon, S.; Wipff, G.; Maignet, B. *J. Phys. Chem.* **1990**, *94*, 6056.
- (37) Soetens, J.-C.; Millot, C.; Chipot, C.; Jansen, G.; Ángyán, J. G.; Maignet, B. *J. Phys. Chem. B* **1997**, *101*, 10910.
- (38) Cho, K.-H.; No, K. T.; Scheraga, H. A. *J. Phys. Chem. A* **2000**, *104*, 6505.
- (39) Nam, K.-Y.; Yoon, J. H.; No, K. T. *Chem. Phys. Lett.* **2000**, *319*, 391.
- (40) Mrabet, N. T.; van den Broeck, A.; van den Brande, I.; Stanssens, P.; Laroche, Y.; Lambeir, A. M.; Matthijssens, G.; Jenkins, J.; Chiadmi, M.; van Tilbeurgh, H.; Rey, F.; Janin, J.; Quax, W. J.; Lasters, I.; De Maeyer, M.; Wodak, S. J. *Biochemistry* **1992**, *31*, 2239.
- (41) Voet, D.; Voet, J. G. *Biochemistry*, 2nd ed.; John Wiley & Sons Inc.: New York, 1999; pp 110–111.